

## **Detection of Intraseasonal Oscillations in SMAP salinity in the Bay of Bengal**

**Bulusu Subrahmanyam<sup>1\*</sup>, Corinne B. Trott<sup>1</sup>, and V. S. N. Murty<sup>2</sup>**

<sup>1</sup>School of the Earth, Ocean, and Environment, University of South Carolina, Columbia, SC 29208, United States.

<sup>2</sup>Council of Scientific and Industrial Research (CSIR) - National Institute of Oceanography Regional Centre, Visakhapatnam, 530 017, India.

\*Corresponding author: BulusuSubrahmanyam(sbulusu@geol.sc.edu)

### **Abstract**

Analysis of Soil Moisture Active Passive (SMAP) mission derived sea surface salinity (SSS) during April 2015-December 2017 in the Bay of Bengal (BoB) shows first revelation of new insight of existence of 30-90 day and 10-20 day period Intraseasonal Oscillations (ISOs) in SSS – all phase-locked during August-December. The seasonal SMAP SSS anomaly (SSSA) minimum (-0.5 to -1.0 psu) occurs in October and exhibits year-to-year variation, while SSSA maximum (0.5 psu) occurs in June during 2015-2017. Interestingly, these ISOs encompass the negative phase of seasonal SSSA minimum (August-December) in a year, and are related to seasonal variations in river discharge and surface freshwater flux (precipitation and evaporation), that in turn are impacted by the climatic events. Wavelet analysis reveals larger amplitude (-0.2 to 0.35 psu) 30-90 day ISO in northern BoB during August-November. The northward propagation of the SSS ISOs would modulate the post-monsoon air-sea interactions across the BoB.

### **Plain Language Summary**

NASA recently launched Soil Moisture Active Passive (SMAP) mission on January 31, 2015 and the data products are available since April 1, 2015. We are able to retrieve sea surface salinity (SSS) from SMAP at a higher horizontal and lesser temporal resolution, and larger swath of 1000 km with higher accuracy, compared to the earlier salinity missions, Aquarius and SMOS. In this manuscript, we showed first time new insight of existence of different Intraseasonal Oscillations (ISOs) in salinity at 30-90 day, 10-20 day periods, and 3-7 day synoptic scale oscillations. It is essential to understand how the BoB responds to these oscillations, which have a direct bearing on the air-sea interaction processes and development and intensification of weather disturbances. These weather disturbances are much impacted by the northward propagation of Madden Julian Oscillations. The summer monsoon over the BoB experiences active-break cycles during June-September. The active phase enhances convection and provides heavy rainfall, while the break phase characterizes with less/scanty rainfall over the BoB and also on the Indian sub-continent. While there are studies on seasonal variability in the oceanic processes based on observations and model simulations, the studies pertaining to ISOs are still sparse due to non-availability of data.

### **Key Points**

- New insight on existence of Intraseasonal Oscillations in SMAP sea surface salinity in the Bay of Bengal.
- Large amplitude in SMAP sea surface salinity at 30-90 day period in northern Bay of Bengal.
- Large seasonal SMAP sea surface salinity variation in northern Bay of Bengal relates to the impacts of ENSO and Indian Ocean Dipole events.

## 1 Introduction

The Indian Ocean intraseasonal oscillations (ISOs) range from 3 to 7 day synoptic oscillations of monsoon trough, 10 to 20 day quasi-biweekly mode associated with westward moving synoptic-scale disturbances, and 30 to 90 day Madden-Julian Oscillations (MJOs) that propagate northward across the Bay of Bengal (BoB) during southwest (SW) monsoon season (June-September) and eastward along the equator (Madden and Julian, 1971, 1972).

The MJO is a mode of intraseasonal variability that affects the tropics through air-sea interactions. Anomalous convective and clear-sky conditions associated with the MJO propagate eastward at  $3\text{-}5\text{ ms}^{-1}$  over the tropical Indian Ocean and Pacific Ocean repetitively with a typical period of 40-50 days. The MJO is responsible for drought and flooding conditions across Indonesia and for varying Indian summer monsoon rainfall. Sikka and Gadgil (1980) suggested that sub-monthly ISOs together with the MJO determine the amplitude and phase of the wet and dry spells of the Asian summer monsoon. Usually the monsoon active-break cycles have 30-60 day period coinciding with the MJO that promotes convection and heavy rainfall during active phases and suppresses convection leading to scanty rainfall over the Indian sub-continent during break phases.

MJOs also affect climatic events such as El Niño/La Niña and Indian Ocean Dipole (IOD) (Saji et al., 1999; Webster et al., 1999). Grunseich et al. (2011) detected MJOs in the Indian Ocean using altimetric sea surface height anomalies, and also studied the MJO-related sea surface salinity (SSS) variations in the Indian Ocean using model simulations. The Dipole Mode Index (DMI) variations during 2015-2017 indicate that a strong positive IOD (pIOD) was developed in 2015, a strong negative IOD (nIOD) in 2016, and weaker IOD in 2017 (<http://www.bom.gov.au>). Chaitanya et al. (2015) reported freshening (decrease of salinity) during 2010-2011 in association with the pIOD event in 2011. Weakened cyclonic circulation in the BoB during pIOD events directly influences variability of the Wyrski Jet and freshwater transport between the equatorial Indian Ocean and BoB (Thompson et al., 2006). Further, enhanced precipitation associated with pIOD events directly freshens the BoB and drives increased riverine discharge (Pant et al., 2015). Evaporation-dominated conditions with anomalously low river discharge into the BoB occur during nIOD events result in higher-salinity conditions (Pant et al., 2015). Akhil et al. (2014) based on modelling study suggested that the saltening phase is also associated with vertical mixing of surface freshwaters with the overlying salt waters.

A prominent "quasi-biweekly" mode (10-20 day period) appears in surface pressure and rainfall over northern BoB, and in rainfall over Bangladesh and northeast India, and is linked to southward

propagation of convective activity east of Tibet (Kikuchi and Wang, 2009; Fujinami et al., 2011; Kikuchi et al., 2012). This mode is an important modulator of south Asian monsoon rainfall (Krishnamurti and Ardanuy, 1980).

It is intriguing to understand the response of BoB to the ISOs (10-90 day period) and what physical processes would be affected by these ISOs. The main objective of this study is to show the effectiveness of using the newly acquired SMAP SSS data during April 2015 – December 2017 to address the existence and variability of ISOs in the BoB, and the region of dominance. The paper is organized as follows. In Section 2, the data and methodology are described. In section 3, the results are discussed on the detection of ISOs and their variability. Section 4 concludes this research.

## **2 Data and Methodology**

### **2.1 Satellite Observations, ECMWF Reanalysis, and HYCOM**

NASA's Soil Moisture Active Passive (SMAP) SSS was collected using L-band radiometry at 1.4 GHz with a swath width of approximately 1000 km (Entekhabiet al., 2010; Fore et al., 2016). Launched on January 31, 2015, SMAP has approximate global ocean coverage of 3 days with an exact orbit repeat cycle of 8 days at a spatial resolution of 0.25°. We used SMAP's version 3.0 product as supplied by NASA/Jet Propulsion Laboratory (<ftp://podaac.jpl.nasa.gov/allData/smap/>), which provides daily SSS data derived from the 8-day running mean from April 1, 2015 to present. Geostrophic surface currents are derived from a gridded data set of merged altimetric observations processed by AVISO and hosted by Copernicus Marine Environment Monitoring Service (CMEMS). This dataset is available daily at 0.25° grids from January 1, 1993 to present (<http://cmems-resources.cls.fr/documents/PUM/CMEMS-SL-PUM-008-032-051.pdf>).

Evaporation data are obtained from the European Centre for Medium-Range Weather Forecasts' (ECMWF) ERA-Interim daily global atmospheric reanalysis at 1° spatial resolution (<http://apps.ecmwf.int/datasets/data/interim-full-daily/levtype=sfc/>; Berrisford et al., 2011). Daily precipitation data are obtained from the Global Precipitation Climatology Project (GPCP) Version 1.2, available at 1° spatial resolution. GPCP precipitation is available through NCAR's Research Data Archive (<https://rda.ucar.edu/datasets/ds728.3/>; Huffman et al., 2016).

We have also used global Hybrid Coordinate Ocean Model (HYCOM) with an equatorial horizontal resolution of 0.04° (1/25° or ~4.5 km) and the HYCOM simulated salinity data are compared with SMAP SSSA to better understand ISOs. HYCOM is a product of the HYCOM Consortium for data-assimilative ocean modeling and is run in real time at the Naval Oceanographic

Office Major Shared Resource Center using atmospheric forcing from the NAVy Global Environmental Model (NAVGEM) (Metzger et al., 2009). The first layer in HYCOM is at 5 m depth.

## 2.2 Filtering Techniques and Wavelet analysis

A Butterworth 4<sup>th</sup> order recursive time filter was applied in this study in order to extract the desired signal of the selected ISOs with periods of 30-90 day and 10-20 day and synoptic scale period of 3-7 day (Krishnamurti and Subrahmanyam, 1982; and Krishnamurtiet al.,2017). We have applied Morlet wavelet analysis (Morlet, 1983) *via* a continuous wavelet transform to determine the temporal variability of SMAP salinity in the BoB. This wavelet transform method can be applied to any time-series to analyze its localized intermittent oscillations (Grinsted et al., 2004).

## 3 Results and Discussion

### 3.1 Year-to-year variation of SMAP SSS in August and October during 2015-17

We have analyzed the processed SMAP SSS daily data in the BoB during April 2015-December 2017. Monthly mean SSS and geostrophic currents are presented for peak SW monsoon (August) and post-SW monsoon (October) months (Figures 1a-f). During August, one would see the confinement of low salinity waters (<30 psu) to northern BoB (Figures 1a-c) and inflow of high salinity surface (>34-35.5 psu) waters from southwestern Bay *via* the Southwest Monsoon Current (SMC) under the influence of SW monsoon winds and dynamics (Murtyet al., 1992; Shankar et al., 2002; Vinayachandran et al., 1999, 2018). The SMC advects high salinity waters of Arabian Sea origin northeastward into central Bay up to 12°N in August of all years (Figures 1a-c). An anticyclonic eddy in the northwestern BoB in August 2015 limits the southward extent of low salinity waters and helps push the northern low salinity waters towards northeast. In August 2015, the high salinity waters are also trapped in an anticyclonic circulation cell in the southwestern Bay and up to east coast of India south of 15°N.

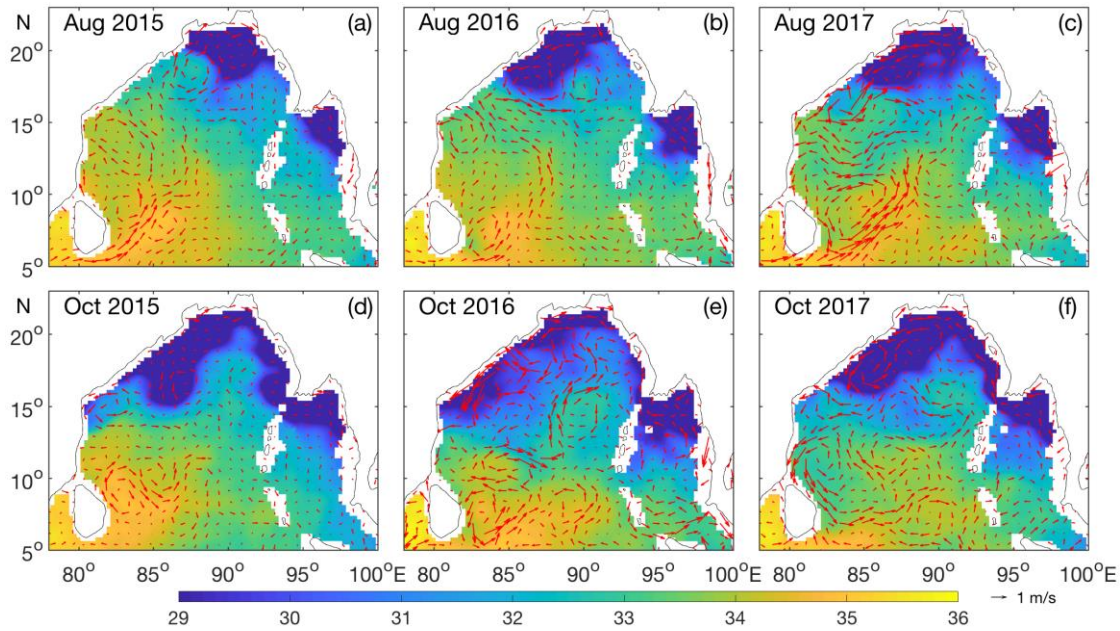


**Figure 1.** Monthly SMAP Sea Surface Salinity (SSS, psu) for the month of August in the years (a) 2015, (b) 2016, and (c) 2017 and the month of October in the years (d) 2015, (e) 2016, and (f) 2017 in the Bay of Bengal. Monthly geostrophic current vectors are superimposed.

In August 2017 the SMC weakens northeastward and continues advection of high salinity waters towards Myanmar coast while cyclonic circulation confines the low salinity waters to the northwestern Bay (Figure 1c). The presence of low salinity waters and the associated warmer SSTs due to stratification in the northwestern Bay in August 2016, 2017 provide intense convection and formation of monsoon depressions. Meridional SSS gradients are large in October along 85°E in 2015, along 88°E in 2016 and along 90°E in 2017, and large zonal SSS gradients are noticed at 18°N in 2015 and 2017. The equatorward flowing East India Coastal Current (EICC) advecting northern low salinity waters southward is weaker in October 2015 (Figure 1d) in association with the pIOD and is stronger up to 15°N in October 2016 and 2017 (Figures 1e-f) in association with the nIOD (Subrahmanyam et al., 2011; Fournier et al., 2017). The observed SMAP SSS in the northern BoB in October 2015 (very low SSS, <30.0 psu) and October 2016 (relatively high SSS, >32.0 psu over a larger area) correspond to the impact of the pIOD and nIOD events (Subrahmanyam et al., 2011; Akhil et al., 2014; Chaitanya et al., 2015).

### 3.2 Wavelet analysis of SMAP SSS anomalies

We have subjected the daily time-series of unfiltered SMAP SSS anomalies (SSSA) to band-pass filtering of period 30-90 day, 10-20 day and 3-7 day and also to the continuous wavelet analysis (Figure 2). The time-series of unfiltered and band-pass filtered SMAP SSSA and the corresponding wavelet spectra are shown in Figures 2a-h. The unfiltered time-series of SSSA shows the dominant

seasonal cycle with large positive SSSA (0.5-0.7 psu) during April-June, prior to the onset of SW monsoon, and with large negative SSSA up to -1.0 psu in October 2015 and 2017 during and following the SW monsoon season (Figure 2a). The amplitude of SSSA decreased with decrease in filtering period (Figures 2e-h). Higher amplitudes of SSSA (-0.2 to +0.35 psu) are associated with the ISO 30-90 day filter in the BoB (Figure 2a). The 30-90 day ISO attains peak spectral energy in October-November 2015, 2016 and 2017 and April-June 2017. This latter peak represents the First-branch of northward propagating ISO (FNISO) convection over the BoB (Li et al., 2013).

In the unfiltered wavelet power spectrum, higher spectral energy occurs at 180 day, 45 day, 14 day and 5 day. In this study, we will highlight only the 45 day, 14 day and 5 day with their range of ISO period 30-90 day and 10-20 day and synoptic period of 3-7 day. The 180-day signal is the semiannual variation potentially signaling the propagation of semiannual Rossby waves in the BoB. The 27 day peak in wavelet energy is not elaborated as its peak energy is closer to the Cone of Influence (Figure 2e). It is interesting to note that the biweekly ISO is also noticed in SSSA with higher amplitudes ( $\pm 0.15$  psu) in October-November 2016, 2017 and in April-June 2017 (Figures 2c, 2g). The amplitudes of 3-7 day oscillations, though generally weak (within  $\pm 0.05$  psu), attain relatively higher values in August-October 2015 (Figures 2d, 2h). It appears that these 3-7 day ISOs modulated the 30-90 day ISO or MJO in October-November 2015 (Figures 2b, 2d) and April-June 2017 and October-November 2017 (Figures 2f, 2h).

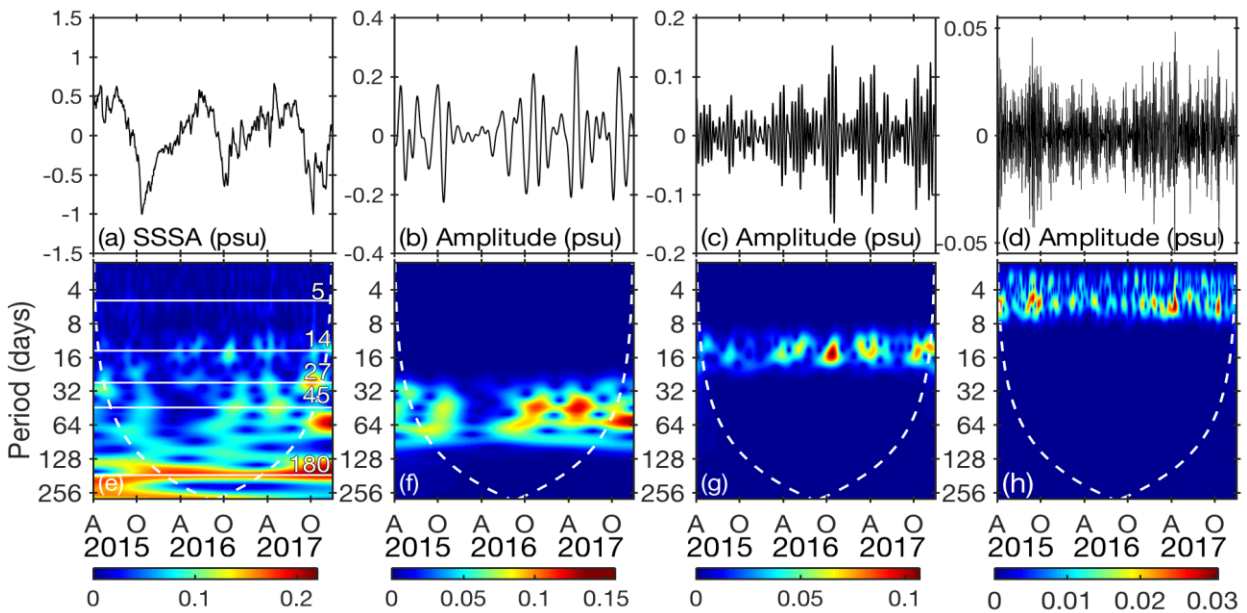


**Figure 2.** Top panel figures (a-d) represent the time-series of the box averaged [85°E-95°E and 4°N-18°N] SMAP SSSA for (a) unfiltered SSSA and filtered SSSA for ISO periods of (b) 30-90 day

and (c) 10-20 day and (d) synoptic oscillation of 3-7 day period and the corresponding bottom panel figures (e-h) represent continuous wavelet power spectrum of the box-averaged time-series in (a-d). The white horizontal lines in (e) denote the periods of peak wavelet power, and the white dotted line in each figure signifies the cone of influence (COI) where edge effects might distort the signal. Along the x-axis, 'A' represents April and 'O' represents October.

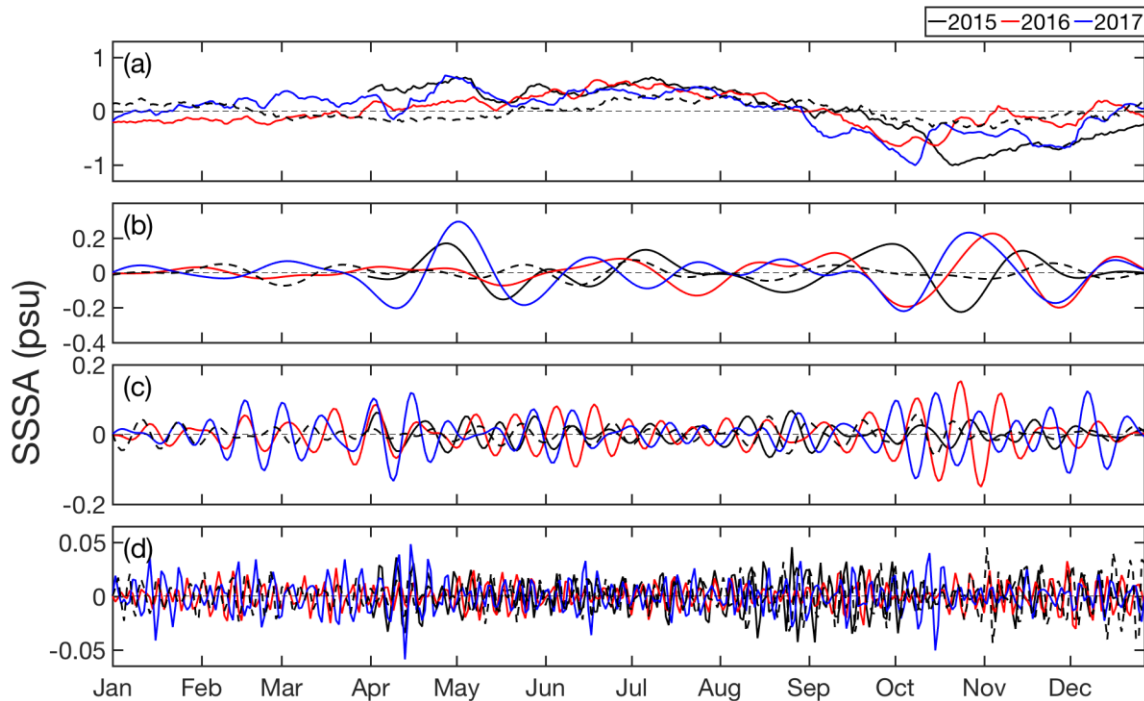


**Figure 3.** Time-series of the 8-day running mean of the deseasonalized daily SMAP (solid lines) and HYCOM (dashed line) sea surface salinity anomalies (SSSA) box-averaged [85°E-95°E and 4°N-18°N] in the years of 2015, 2016 and 2017 for (a) unfiltered SSSA and filtered SSSA for periods of (b) 30-90 day, (c) 10-20 day and (d) 3-7 day in the Bay of Bengal.

### 3.3 Variations of SMAP SSS anomalies for different ISO periods

Here, we also presented HYCOM SSSA to compare the SMAP SSSA in 2015. Figure 3 presents the comparison of annual variations of the box averaged (4°N-18°N and 85°E-95°E) SMAP SSSA amplitudes for the unfiltered and band-pass filtered time series data in 2015 (black), 2016 (red) and 2017 (blue). The annual variation of HYCOM SSSA in the year 2015 at 5 m depth (dashed line) is also included (Figure 3a). The SSSA peaks in synoptic 3-7 day and ISO 10-20 day precede the ISO 30-90 day peaks in April-May and October-November. For the 30-90 day ISO, the SSSA amplitudes are large during September-December, and the SSSA amplitude in 2015 is opposite to that in 2016

and 2017. The biweekly ISO SSSA amplitudes are phase locked (September-December) to those of 30-90 day ISO.

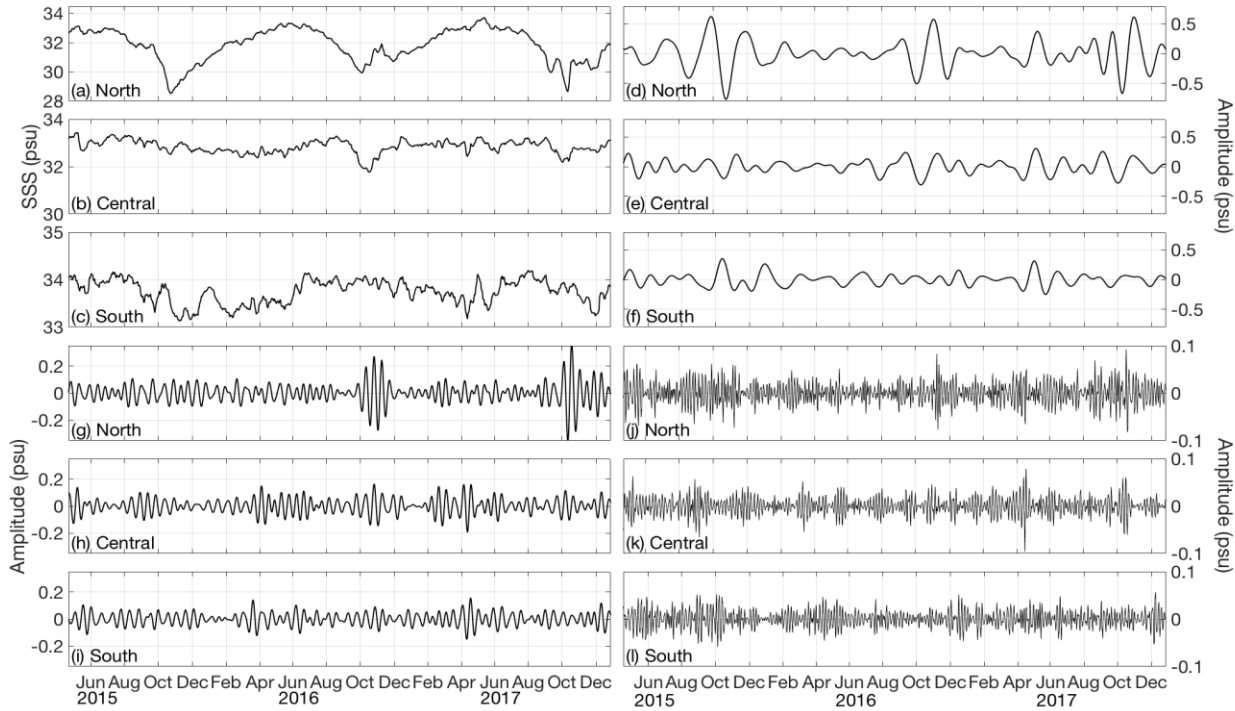


**Figure 4.** Time series of the 8-day running mean daily SMAP SSSA for the northern Bay box ( $14^{\circ}\text{N}$ - $18^{\circ}\text{N}$ ,  $85^{\circ}\text{E}$ - $95^{\circ}\text{E}$ ), Central Bay box ( $10^{\circ}\text{N}$ - $14^{\circ}\text{N}$ ,  $85^{\circ}\text{E}$ - $95^{\circ}\text{E}$ ) and Southern Bay box ( $5^{\circ}\text{N}$ - $10^{\circ}\text{N}$ ,  $85^{\circ}\text{E}$ - $95^{\circ}\text{E}$ ) for (left, **a-c**) unfiltered SSSA and filtered SSSA at periods of (right, **d-f**) 30-90 day, (left, **g-i**) 10-20 day and (right, **j-l**) 3-7 day.

We further examined the SSS variations of the unfiltered and band-pass filtered SMAP SSS in different regions of the BoB (Figure 4). The northern Bay box exhibits a strong seasonal variation with higher SSS in June, prior to the onset of SW monsoon, and lower SSS in October peak precipitation and arrival of river discharge plumes into the northern BoB. The seasonal variation in SSS in the central Bay box is weak and is moderate in the southern Bay box wherein high salinity waters enter the BoB during SW monsoon through the SMC. The annual variation of SSS is about 5 psu in the northern Bay box from October 2015 to June 2016, and is about 3.5 psu from October 2016 to June 2017 and this large SSS variation is associated with the variations in the magnitude of riverine flux of Ganges-Brahmaputra (GB) river system (Papa et al., 2010; Papa et al., 2012) and with the variations in freshwater flux (Precipitation minus Evaporation).

The northward propagation of ISOs with 30-90 day period prior to and during the SW monsoon might bring large variations in the freshwater flux from one year to the other year. Based on Oceanic



Niño Index (ONI) (<http://www.cpc.ncep.noaa.gov>), 2014-15 was a weak El Niño, 2015-16 was a very strong El Niño, and 2016-17 was a weak La Niña (McPhaden, 2015; Corbett and Subrahmanyam, 2016). El Niño-Southern Oscillation (ENSO) events directly impact the salinity variability in the BoB by shifting the regions of anomalous precipitation as described in Ashok et al. (2004). During 2014-17 strong pIOD and nIOD events and weaker IOD event also occurred. Very low salinity (28.5 psu) waters in October 2015, 2017 can be attributed to the freshening phase due to strong pIOD event in 2015 and weaker El Niño of 2014-15 and to weak IOD in 2017 and La Niña of 2016-17. Similarly, the relatively higher low salinity (~30 psu) waters in October 2016 are related to the strong nIOD and El Niño of 2015-16.

Thus the satellite observations of SMAP SSS in the northern BoB captured the impact of GB discharge variations associated with ENSO and IOD events during 2015-2017. This highlights that the strongest peaks in the northernmost BoB are due to seasonal cycle variations in riverine discharge and surface freshwater flux. The northern BoB responds to the MJO events as evident *via* the strongest 30-90 day signal around October of 2015, indicating a strong seasonal interaction of the northern BoB with the atmospheric MJOs and low frequency ISOs.

In the 10-20 day ISO signal, there is a marginal difference in peak amplitude between the northern, central, and southern BoB. The peak 10-20 day ISO in the northern BoB occurs in October following the SW monsoon and has the largest amplitude among the three regions. The peak shifts to April in the central BoB and to April and June in southern BoB.

Unlike the ISOs with longer periods, the amplitudes of the peaks in the synoptic 3-7 day signal are consistent between the northern, central, and southern BoB. There is a strong October pulse in the northern BoB and central BoB.

#### 3.4 Propagation of SMAP SSS ISO signals in the Bay of Bengal during 2015-17

The time-latitude Hovmöller diagrams for the SMAP SSS anomaly for each ISO and synoptic oscillation signal in each year show meridional propagation and variability across the BoB (Figures 5a-c). The northward propagation of negative SSS anomalies coincide with that of convection spells in association with the 30-90 day period ISOs. In Figure 5a, the northward propagation of SSSA is evident in the 30-90 day ISO during April-May 2015 and 2017, possibly related to the FNISO prior to the onset of SW monsoon (Li et al., 2013), which is absent or weak in April-May 2016. It is important to note the differences in the amplitude and timing of 30-90 day ISOs in SSS in the BoB. Generally, basin-wide ISOs are weak from December through March.

During the rest of the year, higher-amplitude ISOs are consistently found in the northern BoB with a poleward-moving signal.

In the 10-20 day quasi-biweekly signal, northward propagation of ISOs is more easily seen, particularly prior to and following the SW monsoon season, and the highest amplitude ISO occurs in October 2016. The winter and summer monsoon seasons show the smallest basin-wide amplitudes of 10-20 day ISO in SMAP SSS. In 2015 and 2017, this ISO propagates southward from August to November from the northern Bay to central Bay, and northward propagation from southern Bay to central Bay. This discrepancy in this quasi-biweekly ISO in SSS from the central Bay to northern Bay might be due to the convection and the associated precipitation under the influence of the dominant westward movement of the synoptic weather disturbances across the BoB.

Unlike the propagation of low frequency ISOs (Figures 5a,b), there is consistent pattern of poleward propagation in the synoptic 3-7 day signal from April-May and October-December of 2015, 2016 and 2017. The amplitude of this ISO signal is weak, compared to the other low frequency ISOs.

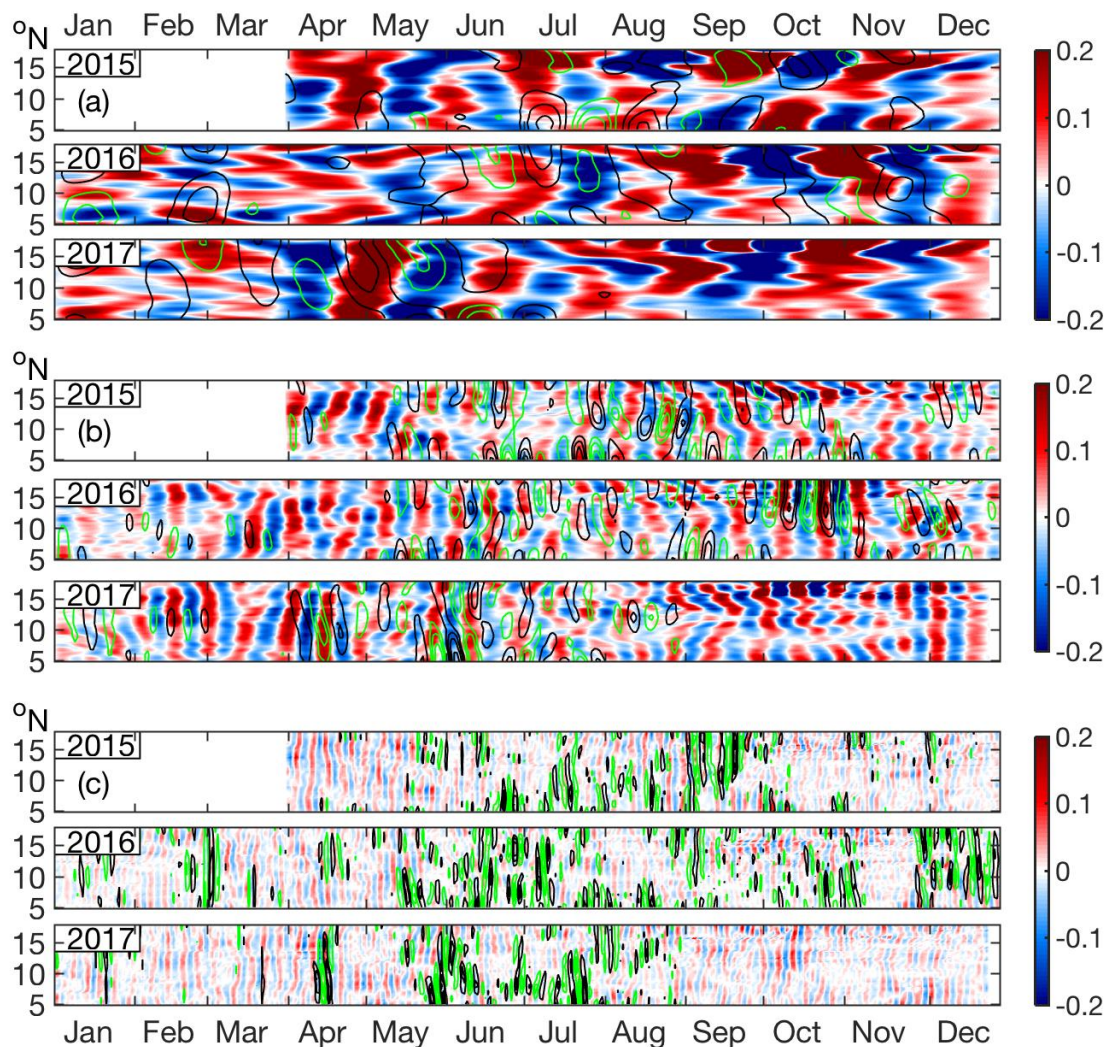


**Figure 5.** Time-latitude Hovmöller diagrams of daily SMAP (using 8-Day running mean, fill) and daily SSSA (psu) longitudinally averaged over 85°E-95°E in the Bay of Bengal in the years 2015, 2016 and 2017 for the filtered SSSA at periods of (a) 30-90 day, (b) 10-20 day and (c) 3-7 day. Green contours are negative GPCP precipitation minus ECMWF evaporation (P-E) and black contours are positive P-E values, and contour interval is every 4 mm/day.

#### 4 Conclusions

As far as of our best knowledge, this is the first study in the BoB using SMAP salinity data during 2015-2017 to detect the ISOs in SSS of period 30-90 day and 10-20 day and synoptic oscillations of period 3-7 day and identifies the ability of NASA's SMAP mission to accurately detect these ISOs and synoptic oscillations in SSS. Accurate SSS observations collected by the SMAP mission at the current spatial coverage and duration are unprecedented. The ISOs of 30-90 day period have been detected in Aquarius salinity (Grunseichet al., 2013), but here we show the existence of ISOs in SSS with 30-90 day and 10-20 day period and synoptic oscillations (3-7 day period) in the BoB using SMAP salinity data. This study deciphers well the uniqueness of the northern BoB with the observed large seasonal variation in SSS, as influenced by the ENSO and IOD events and higher amplitude ISOs of 30-90 day and 10-20 day quasi-biweekly periods. We envisage that the measurements gathered from this mission will broaden our understanding on the role of these SSS ISOs on the SST variability at intraseasonal time scales and its impact on the upper ocean monsoon dynamics and air-sea interactions that include the active and break monsoon cycles over the BoB.

#### Acknowledgments

This work is supported by the ONR's Oceanic Control of Monsoon Intra-seasonal Oscillations in the Tropical Indian Ocean and the Bay of Bengal (MISO-BOB) Award number N00014-17-1-2468 awarded to BS. The author, VSNM, is thankful to the Scientist-in-Charge of CSIR-NIO Regional Centre and Director, CSIR-NIO for their keen interest in the joint-collaborative research with BS at the University of South Carolina, Columbia, USA. SMAP V3.0 data are produced by Remote Sensing Systems and is available through JPL/PODAAC. Archiving Validation and Interpretation of Satellite Oceanographic data (AVISO) were obtained from [www.aviso.oceanobs.com](http://www.aviso.oceanobs.com). ECMWF ERA-Interim daily data can be found at <http://apps.ecmwf.int/datasets/data/interim-full-daily/levtype=sfc/> and the daily GPCP data can be downloaded from NCAR's Research Data Archive at <https://rda.ucar.edu/datasets/ds728.3/>. This has the NIO contribution number xxxx.

## References

- Akhil, V. P., Fabian Durand, Matthieu Lengaigne, J. Vialard, M. G. Keerthi, V. V. Gopala Krishna, Charles Deltel, Fabrice Papa, & C. de Boyer Montegut (2015), A modelling study of the processes of surface salinity seasonal cycle in the Bay of Bengal, *J. Geophys. Res.*, doi:10.1002/2013JC009632.
- Ashok, K., Guan, Z., Saji, N. H., & Yamagata, T. (2004), Individual and combined influences of ENSO and the Indian Ocean dipole on the Indian summer monsoon. *J. Clim.*, 17(16), 3141-3155.
- Berrisford, P., Källberg, P., Kobayashi, S., Dee, D., Uppala, S., Simmons, A. J., et al. (2011), Atmospheric conservation properties in ERA-Interim. *Quarterly Journal of the Royal Meteorological Society*, 137(659), 1381-1399.
- Chatterjee, P., & Goswami, B. N. (2004), Structure, genesis and scale selection of the tropical quasi-biweekly mode. *Quart. J. Royal Meteorol. Soc.*, 130(599), 1171-1194.
- Chaitanya A.V.S., Durand, F., Mathew, S., Gopalakrishna, V. V., Papa, F., Lengaigne, M., et al. (2015), Observed year-to-year sea surface salinity variability in the Bay of Bengal during the 2009 – 2014 period. *Ocean Dyn.*, 65(2), 173-186.
- Corbett, C.M., & Subrahmanyam, B. (2016), Validation of Satellite-Derived Salinity in the Equatorial Pacific with Specific Emphasis on the 2014–15 ENSO Event. *IEEE Geos. and Remote Sens. Letts.*, 13 (12), 1979-1983. doi:10.1109/LGRS.2016.2619980.
- Entekhabi, D., Njoku, E. G., O'Neill, P. E., Kellogg, K. H., Crow, W. T., Edelstein, W. N., et al. (2010), The soil moisture active passive (SMAP) mission. *Proc. IEEE*, 98(5), 704-716.
- Fore, A. G., Yueh, S. H., Tang, W., Stiles, B. W., & Hayashi, A. K. (2016), Combined active/passive retrievals of ocean vector wind and sea surface salinity with SMAP. *IEEE Trans. Geos. and Remote Sens.*, 54(12), 7396-7404.
- Fournier, S., Vialard, J., Lengaigne, M., Lee, T., Gierach, M. M., & Chaitanya, A. V. S. (2017), Modulation of the Ganges-Brahmaputra River Plume by the Indian Ocean Dipole and Eddies Inferred From Satellite Observations. *J. Geophys. Res. Oceans*, 122, 9591-9601.
- Fujinami, H., Hatsuzuka, D., Yasunari, T., Hayashi, T., Terao, T., Murata, F., et al. (2011), Characteristic intraseasonal oscillation of rainfall and its effect on interannual variability over Bangladesh during boreal summer. *Int. J. Climatol.*, 31(8), 1192-1204.
- Grinsted, A., Moore, J. C., & Jevrejeva, S. (2004), Application of the cross wavelet transform and wavelet coherence to geophysical time series. *Nonlinear Processes in Geophysics*, 11(5/6), 561-566.
- Grunseich, G., Subrahmanyam, B., & Arguez, A. (2011), Influence of the Madden-Julian Oscillation on sea surface salinity in the Indian Ocean. *Geophys. Res. Lett.*, 38(17).
- Grunseich, G., Subrahmanyam, B., & Wang, B. (2013), The Madden-Julian oscillation detected in Aquarius salinity observations. *Geophys. Res. Lett.*, 40(20), 5461-5466.

- Han, W., Yuan, D., Liu, W. T., & Halkides, D. J. (2007), Intraseasonal variability of Indian Ocean sea surface temperature during boreal winter: Madden-Julian Oscillation versus submonthly forcing and processes. *J. Geophys. Res.: Oceans*, 112(C4).
- Huffman, G. J., Bolvin, D. T., & Adler, R. F. (2016), GPCP version 1.2 one-degree daily precipitation data set. *Research Data Archive at the National Center for Atmospheric Research, Computational and Information Systems Laboratory, Boulder, Colo.*, doi, 10, D6D50K46.
- Kiladis, G. N., & Weickmann, K. M. (1997), Horizontal structure and seasonality of large-scale circulations associated with submonthly tropical convection. *Mon. Weather Rev.*, 125(9), 1997-2013.
- Kikuchi, K., & Wang, B. (2009), Global perspective of the quasi-biweekly oscillation. *J. Clim.*, 22(6), 1340-1359.
- Kikuchi, K., Wang, B., & Kajikawa, Y. (2012), Bimodal representation of the tropical intraseasonal oscillation. *Clim. Dyn.*, 38(9-10), 1989-2000.
- Krishnamurti, T. N., & Ardanuy, P. (1980), The 10 to 20-day westward propagating mode and "Breaks in the Monsoons". *Tellus*, 32(1), 15-26.
- Krishnamurti, T. N., Jana, S., Krishnamurti, R., Kumar, V., Deepa, R., Papa, F., et al. (2017), Monsoonal intraseasonal oscillations in the ocean heat content over the surface layers of the Bay of Bengal. *J. Marine Sys.*, 167, 19-32.
- Krishnamurti, T. N., & Subrahmanyam, D. (1982), The 30–50 day mode at 850 mb during MONEX. *J. Atmos. Sci.*, 39(9), 2088-2095.
- Lawrence, D. M., & Webster, P. J. (2002), The boreal summer intraseasonal oscillation: Relationship between northward and eastward movement of convection. *J. Atmos. Sci.*, 59(9), 1593-1606.
- Li, K, Yu, W., Li, T., Murty, V.S.N., Khokiattiwong, S., Adi, T. R., et al. (2013), Structures and mechanisms of the first-branch northward-propagating intraseasonal oscillation over the tropical Indian Ocean. *Clim. Dyn.*, 40, 1707-1720. DOI 10.1007/s00382-012-1492-z.
- Madden, R. A., & Julian, P. R. (1971). Detection of a 40–50 day oscillation in the zonal wind in the tropical Pacific. *J. Atmos. Sci.*, 28(5), 702-708.
- Madden, R. A., & Julian, P. R. (1972), Description of global-scale circulation cells in the tropics with a 40–50 day period. *J. Atmos. Sci.*, 29(6), 1109-1123.
- McPhaden, M. J. (1999), Genesis and evolution of the 1997-98 El Niño. *Science*, 283(5404), 950-954.
- McPhaden, M. J. (2015), Playing hide and seek with El Niño. *Nature Climate Change*, 5, 791–795.
- Metzger, E.J., H.E. Hurlburt, A.J. Wallcraft, O.M. Smedstad, J.A. Cummings, & E.P. Chassignet (2009), Predicting "Ocean Weather" Using the HYbrid Coordinate Ocean Model (HYCOM), NRL Review, Washington DC, 202-206.

- Morlet, J. (1983), Sampling theory and wave propagation. In *Issues in acoustic Signal—image processing and recognition* (pp. 233-261). Springer, Berlin, Heidelberg.
- Murakami, T. (1976), Cloudiness fluctuations during the summer monsoon. *J. Meteorol. Soc. of Japan. Ser. II*, 54(3), 175-181.
- Murty, V.S.N., Sarma, Y. V. B., & Rao, D. P. (1996), Variability of the Oceanic boundary layer characteristics in the northern Bay of Bengal during MONTBLEX-90, *Proc. Indian Acad. Sci. (Earth and Planet. Sci.)*, 105, 41–61.
- Pant, V., Girishkumar, M. S., UdayaBhaskar, T. V. S., Ravichandran, M., Papa, F., & Thangaprakash, V. P. (2015), Observed interannual variability of near-surface salinity in the Bay of Bengal. *J. Geophys. Res. (Oceans)*, 120(5), 3315-3329, doi:10.1002/2014JC010340.
- Papa, F., Durand, F., Rossow, W. B., Rahman, A., & Bala, S. K. (2010), Satellite altimeter-derived monthly discharge of the Ganga-Brahmaputra River and its seasonal to interannual variations from 1993 to 2008. *J. Geophys. Res. (Oceans)*, 115(C12), doi:10.1029/2009JC006075.
- Papa, F., Bala, S. K., Pandey, R. K., Durand, F., Gopalakrishna, V. V., Rahman, A., et al. (2012), Ganga-Brahmaputra river discharge from Jason-2 radar altimetry: An update to the long-term satellite-derived estimates of continental freshwater forcing flux into the Bay of Bengal. *J. Geophys. Res. (Oceans)*, 117(C11), doi:10.1029/2012JC008158.
- Rao, S.A., & Yamagata, T. (2004), Abrupt termination of Indian Ocean Dipole events in response to intraseasonal disturbances. *Geophys. Res. Lett.* 31, L19306, doi:10.1029/2004GL020842.
- Saji, N. H., Goswami, B. N., Vinayachandran, P. N., & Yamagata, T. (1999), A dipole mode in the tropical Indian Ocean. *Nature*, 401(6751), 360.
- Sengupta, D., Goswami, B. N., & Senan, R. (2001), Coherent intraseasonal oscillations of ocean and atmosphere during the Asian summer monsoon. *Geophys. Res. Lett.*, 28(21), 4127-4130.
- Shankar, D., Vinayachandran, P. N., & Unnikrishnan, A.S. (2002), The monsoon currents in the north Indian Ocean. *Prog. Oceanogr.*, 52, 63–120, doi:10.1016/S0079-6611(02)00024-1.
- Sikka, D. R., & Gadgil, S. (1980), On the maximum cloud zone and the ITCZ over Indian, longitudes during the southwest monsoon. *Mon. Weather Rev.*, 108(11), 1840-1853.
- Subrahmanyam, B., Murty, V.S.N., & Heffner, D. (2011), Sea surface salinity variability in the tropical Indian Ocean, *Remote Sens. Environ.*, 115, 944-956.
- Thompson, B., Gnanaseelan, C., & Salvekar, P. S. (2006), Variability in the Indian Ocean circulation and salinity and its impact on SST anomalies during dipole events. *J. Mar. Res.*, 64(6), 853-880.
- Vinayachandran, P. N., Masumoto, Y., Mikawa, T. & Yamagata, T. (1999), Intrusion of the southwest monsoon current into the Bay of Bengal. *J. Geophys. Res.*, 104 (C5), 77–85.
- Vinayachandran, P. N., Matthews, A. J., Vijay Kumar, K., Sanchez-Franks, A., Thushara, V., George, J., et al. (2018), BoBBLE (Bay of Bengal Boundary Layer Experiment): Ocean–

atmosphere interaction and its impact on the South Asian monsoon. *Bull. Am. Meteorol. Soc.*, doi:10.1175/BAMS-D-16-0230.1.

Webster, P. J., Moore, A. M., Loschnigg, J. P., & Leben, R. R. (1999), Coupled ocean–atmosphere dynamics in the Indian Ocean during 1997–98. *Nature*, 401(6751), 356.

Wheeler, M. C., & Hendon, H. H. (2004), An all-season real-time multivariate MJO index: Development of an index for monitoring and prediction. *Mon. Weather Rev.*, 132(8), 1917-1932.